# Some Remarks on the Neutronics of Spallation Targets

W.E. Fischer
Swiss Institute for Nuclear Research, CH - 5234 Villigen, Switzerland

B. Sigg
Institute for Reactor Technology, CH - 5303 Würenlingen, Switzerland



## Introduction

Target-reflector neutronics should provide us with energy and spatial distribution of the neutrons in the proximity of the spallation target. The time distribution is not essential for a continuous source and will not be considered in this paper. These investigations are usually performed with Monte-Carlo codes, e.g. HETC. A "black box" application of such codes may however be dangerous, involved
and time consuming, especially for parametric studies. We therefore prefer some preparatory investigations preceding the application of the Monte-Carlo codes. This preparation consists of an educated guess as a first step, followed by a one-dimensional diffusion calculation furnishing physical insight into trends of parametric behaviour. In this paper we shall present a few typical examples related to the project of the SIN-spallation neutron source.

1) Inelastic Moderation of Evaporation Neutron Spectra in a Heavy Metal Target.

2) Neutron Multiplication due to (n, 2n)-Reactions in a Beryllium Reflector.

3) Neutron Multiplication due to Fast Fission in a Depleted Uranium Target.

The basic geometry in all these examples is quite simple: a cylinder-target embedded into cylindric moderators and reflectors. Where ever available, we use experimental data as input describing the nuclear physics in the target.

## 1) Inelastic Moderation of Evaporation Neutrons

### a) Energy Loss of Evaporation Neutrons

Let $\Sigma(u)$ be the macroscopic inelastic cross section for neutron scattering depending on the lethargy u.
$\Delta u_1 = u_i - u_{i-1}$ are the group intervals
$f(u', u-u')$ is the scattering probability for an inelastic nuclear scattering, shifting the neutron lethargy from u', → u. The group cross section $\Sigma^{k\to i}$ is then defined by

$$\Sigma^{k\to i} = \frac{1}{\Delta u_k} \int_{u_{k-1}}^{u_k} \Sigma(u')\, du' \int_{u_{i-1}}^{u_i} f(u', u-u')\, du \qquad (1)$$

The first integral represents the average inelastic cross section $\bar{\Sigma}(k)$ of neutrons in group k. The second one expresses the probability $P(k\to i)$ of scattering into group i. These data are available for several possible target and reflector materials[1]. In order to obtain an idea of the moderating power of different materials we have calculated the energy transfer

$$E^{k\to i} = (\bar{E}_k - \bar{E}_i)\, \bar{\Sigma}(k)\, P(k\to i) \qquad (2)$$

and particularly the average energy loss for neutrons from different relevant groups

$$\frac{d\bar{E}}{dx}(E_k) = \sum_{i=k+1}^{N} (\bar{E}_k - \bar{E}_i)\, \bar{\Sigma}(k)\, P(k\to i) \ [\mathrm{MeV/cm}] \qquad (3)$$

$E_k$ or rather $dE/dx\,(E_n)$ is shown in Fig. 1 for Pb, Be, C and $D_2$ in the energy interval 1 to 15 MeV. For the light elements the energy loss due to elastic scattering alone is also indicated.



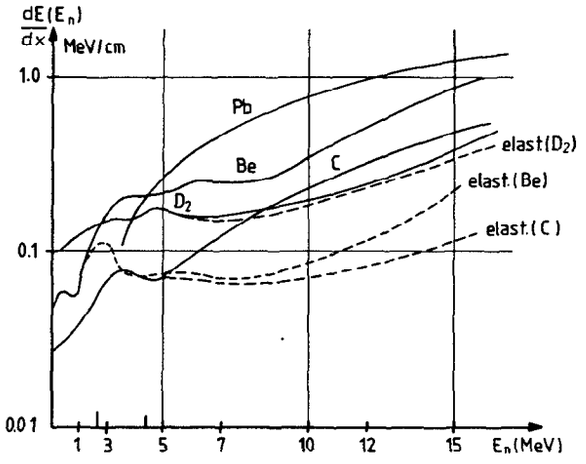


Fig. 1
Stopping power of evaporation neutrons in various target and reflector materials

We see that lead has the highest stopping power among all these moderators for neutrons with $E_n > 4$ MeV. Since the average energy of the primary spectrum of evaporation neutrons is somewhat larger than 4 MeV and the absorption cross section is low, even down to thermal energies, lead is a good moderator for such hard spectra. The same is certainly also true for bismuth. Furthermore the self-shielding property of lead and bismuth for γ-rays is obvious.

The moderation property of lead should be considered also in the interpretation of spectra measured at the bare target. Even if the primary evaporation spectrum is strictly isotropic, this isotropy will be destroyed in a thick target by inelastic moderation. Hence angular dependence of the evaporation part of the neutron spectra will be observed[2].

In order to obtain a quantitative idea on the distortion of the spectrum we carried out the following transport calculation. We start with an evaporation spectrum

$$W(E) = \frac{2}{\sqrt{\pi}} \frac{E^{1/2}}{T^{3/2}} C^{-E/T} \quad \text{with } T = 2.6 \text{ MeV} \qquad (4)$$

Transport of (4) through 1.3 cm of lead reproduces fairly well the leakage spectrum from a lead target with R = 1.3 cm obtained by Monte-Carlo method[3]. This spectrum is already deformed and cannot be described anymore by (4). With the one-dimensional ANISN-code we transport this spectrum through (infinitly long) lead cylinders of various radii. The calculation is done in $S_8$-approximation considering $P_0$,$P_1$-scattering and 15 energy groups. We assumed a rectangular beam profile with 5 cm diameter. The leakage spectra for targets with radii $R_T$ = 5 and 10 cm are shown in Fig. 2. The moderation by the extra 5 cm-layer of lead is evident. The spectral content for energies $E_n > 4$ MeV is roughly halved. The average energy drops from 2.86 MeV to 2.06 MeV.

From Fig. 1 we realize that this softer spectrum is now most efficiently moderated further by beryllium. Since many neutrons are still above the (n,2n)-reaction threshold ($E \gtrsim 2.7$ MeV) we expect moreover some multiplication of neutrons in a Be-sleeve.

## 2) Neutron Multiplication in a Beryllium Reflector

*In this chapter we would like to estimate the neutron multiplication due to (n,2n) reactions in a Be-sleeve.*

### a) Geometry - Average Chord Length

In Fig. 3 the geometry of the target-sleeve arrangement is shown. The chord length $S(\rho,\theta)$ averaged over target cross section and



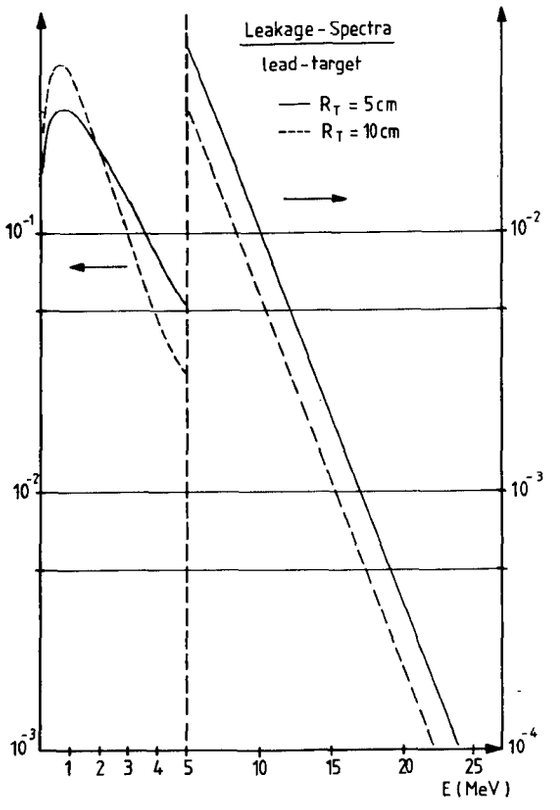


Fig. 2
Leakage spectra from a lead target with 5.0 and 10 cm radius

all plane directions θ is for r/R = 1/2

$$\bar{S} = 1.12\ r \qquad (5)$$

where r is the target radius and R the radius of the Be-sleeve.

For the estimate of the average path length in the beryllium we refer to Fig. 3b. For simplicity we assume a disk-source, 6 cm behind the target front face. From Rh-foil measurements on the surface of a lead target, we know that this is the

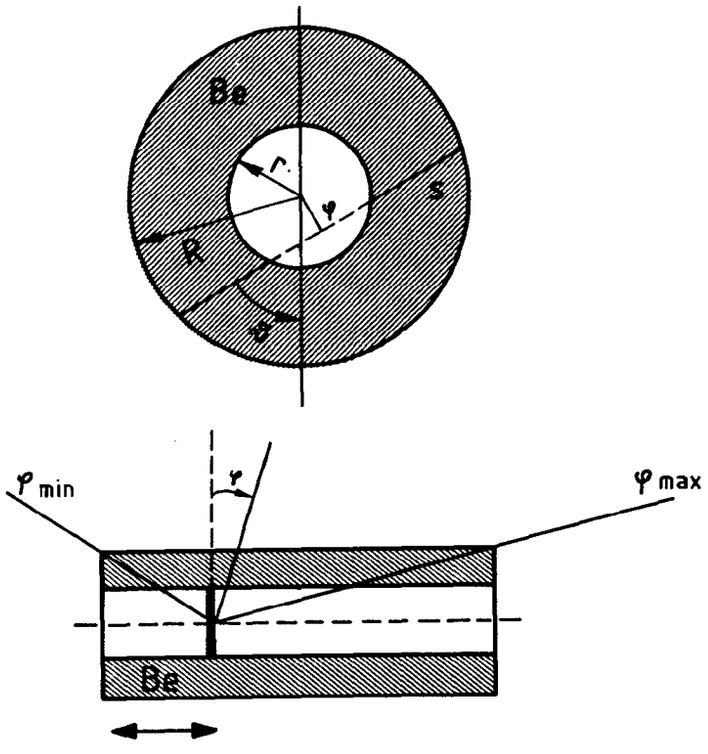


Fig. 3
Sketch of the target
beryllium sleeve geometry

position of maximal source strength for a 590 MeV proton beam. This is indeed a very rough approximation, but one may realize that the average path length is not very sensitive to this position and therefore also not to the exact source distribution.

With a macroscopic scattering cross-section Σ we obtain for the (no scattering) escape probability



$$P_o = \frac{\int_{\phi min}^{\phi max} \exp[-\bar{S}(\frac{R-r}{r}) \frac{\Sigma}{\cos\phi}]^{d(\sin\phi)}}{\int_{\phi min}^{\phi max} d(\sin\phi)} \qquad (6)$$

The cross sections used in this formula should be averaged over the leakage spectrum from the corresponding target. We shall use here the spectrum from a 10 cm lead target (590 MeV protons) measured under 90° by time-of-flight technique at SIN[2] (Fig. 4).

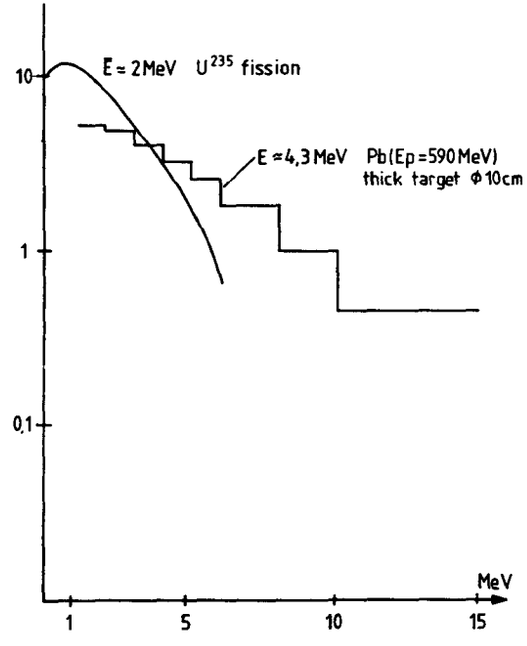


Fig. 4
Experimental TOF-spectrum of evaporation neutrons from a 10 cm diameter lead target, produced by a 590 MeV proton beam. For comparison a $^{235}U$-fission spectrum is also shown.

According to chapter 1 this is the angular region with the hardest leakage spectrum. The multiplication figures we shall obtain, will therefore be somewhat overestimated.

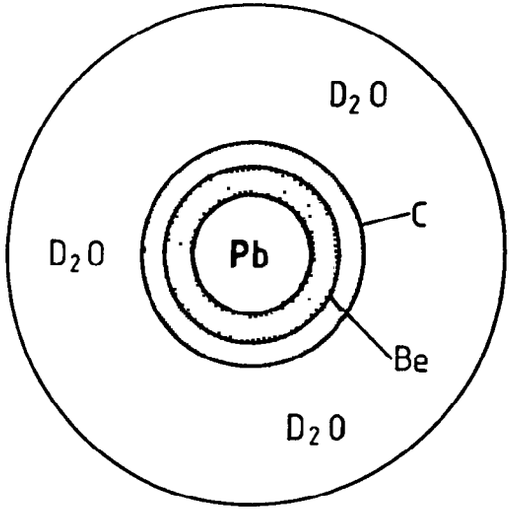


Fig. 5
Schematic target-containment-reflector arrangement for the proposed SIN-neutron source (we still believe in a carbon or beryllium containment for the lead-bismuth eutecticum).

The following values are obtained:

$\bar{\Sigma}_{tot} \approx 0.25\ cm^{-1}$ $\qquad$ $P_0 = 0.17$

$\frac{\bar{\Sigma}\ (n,2n)}{\bar{\Sigma}_{(tot)}} \approx 0.23$ $\qquad$ $\frac{\bar{\Sigma}(elast.)}{\bar{\Sigma}(tot)} \approx 0.77$

The collision probability is therefore 83 %.

b) Multiplication Tree

We follow now the neutrons a few collision generations through the Be-sleeve. We simplify this process with the help of two assumptions

i) First flight and first elastic collision lead to a homogeneous neutron distribution;



ii) After two elastic collisions the neutrons are scattered below the (n,2n) threshold.

The first assumption gives us the possibility to use, after the first collision the escape probabilities tabulated in Case et al.[4]. For r = 5 cm and R = 10 cm - $P_c$ = 0.65. If assumption ii) is valid we can stop the procedure after the second generation. We obtain the following result: If a neutron leaves the target with an energy above (n,2n) threshold the probabilities of events in beryllium are

| | |
|---|---|
| Escape (E > 2.7 MeV) | 0.39 |
| Escape degraded (E < 2.7 MeV) | 0.32 |
| (n,2n) | 0.29 |

Since 60 % of all evaporation neutrons in our spectrum are above (n,2n)-threshold we obtain an increase of source strength by beryllium of 17 %.

We expect of course that the efficiency of a beryllium sleeve depends strongly on the hardness of the leakage neutron spectrum. Indeed if we consider the Monte-Carlo spectrum[3] of LA-4789 from lead, which is softer ($\bar{E} \approx 3.25$ MeV) we obtain the following situation

| | |
|---|---|
| Escape (E > 2.7 MeV) | drops |
| Escape degraded (E < 2.7 MeV) | increases |
| (n,2n) | roughly the same |

Since in this spectrum only 32 % of the source neutrons are above threshold the multiplication efficiency decreases to < 10 %. We therefore meet a competitive situation between target thickness and efficiency of neutrons multiplication in the beryllium sleeve. Let us analyze this situation with a corresponding diffusion calculation in the one-dimensional cylindrical geometry sketched in Fig. 5. The calculation starts

with a primary evaporation spectrum (4) with the same nuclear temperature (T = 2.6 MeV) and proceeds with nine energy groups. The results are shown in Table I.

Table I

| Material, Thickness (cm) | | | | Total Leakage of Thermal Neutrons per Source Neutron | Flux at Outer C-Surface |
|---|---|---|---|---|---|
| Pb | Be | C | $D_2O$ | | |
| 10 | 0 | 6 | 90 | 0.634 | 0.172 |
| 7.5 | 2.5 | 6 | 90 | 0.704 | 0.204 |
| 5 | 5 | 6 | 90 | 0.776 | 0.239 |
| 10 | 5 | 6 | 85 | 0.651 | 0.172 |
| 7.5 | 5 | 6 | 87.5 | 0.712 | 0.203 |
| 5 | 5 | 6 | 90 | 0.776 | 0.239 |

In the first part of Table I we recognize a 11 % increase of the total leakage of thermal neutrons per source neutron for extra 2.5 cm layers of beryllium. The thermal flux at the outer carbon surface rises somewhat stronger, indicating the more efficient moderation by berylllium compared to lead. This would not necessarily be the case, if we had chosen a harder source spectrum.

In the second part of Table I we have just added 5 cm Be-layers to targets of various thicknesses. Compare now the flux at the outer carbon surface of the two parts in the Table, e.g. 10 cm target and 0 and 5 cm Be respectively. We recognize that the gain in source strength due to 5 cm beryllium approximately compensates the flux corresponding radial drop in the $D_2O$ reflector. This is certainly only valid in the proximity of the source.

We have also verified a smaller gain due to the beryllium sleeve by interchanging the carbon with the beryllium layers in this geometry. Obviously the neutron spectrum entering into the beryllium becomes too soft in the carbon for an efficient (n,2n)-gain.



## 3) Neutron Multiplication Due to Fast Fission in a Depleted Uranium Target

Since we want to consider the finite length of the target in this subject, we should first obtain an idea on the longitudinal distribution of the source of primary spallation neutrons. Concerning these primary neutrons we do not distinguish between evaporation- and fission neutrons from spallation isotopes. We are interested here in the multiplication of the source neutrons by their internuclear cascade in a thick uranium target. We treat the longitudinal source distribution by a cascade model of Barbier et al.[5].

### a) Longitudinal Cascade Model

Let $N_n(z)$ be the number of fast cascade nucleons produced in $n^{th}$ generation at depth z. The total number of cascade nucleons is

$$N(z) = \sum_n N_n(z) \qquad z > 0 \tag{7}$$

The longitudinal cascade is ruled by the following equation:

$$dN_n(z) = \lambda^{-1} M_n N_{n-1}(z)dz - \lambda^{-1} N_n(z)dz \tag{8}$$

where

$M_n$ : multiplicity for creation of fast cascade nucleons

$\lambda$ : $A/N_o \cdot \sigma \cdot \rho$(cm) relaxation length in the target material.

Using the relaxation length as length unit ($\zeta = z/\lambda$) we obtain for (8):

$$\frac{dN_U(\zeta)}{d\zeta} + N_n(\zeta) = M_n N_{n-1}(\zeta) \tag{9}$$

$N_o(\zeta) = e^{-\zeta}$ for an exponentially attenuated beam. The general solution is

$$N_n(\zeta) = \pi_n \frac{\zeta^n}{n!} e^{-\zeta} \quad \text{with} \quad \pi_n = \prod_{i=1}^{M} M_n \tag{10}$$

From experiments at thin heavy metal targets we know that 600 MeV protons produce ∿ 5 cascade nucleons. 10 % of them have an energy E > 300 MeV and are therefore still fertile for further cascade reactions. The multiplicity of fertile nucleon production in first generation is therefore $M_1 = 0.5$. We agree that the limit of 300 MeV for possible cascade mechanism is somewhat arbitrary.

For a beam energy of 600 MeV, consideration of 1 to 2 generations is presumably enough - let us for simplicity consider one generation only. Then

$$N(\zeta) = e^{-\zeta}(1+0.5\,\zeta) \simeq e^{-z/\lambda_{eff}} \qquad \lambda_{eff} > \lambda \tag{11}$$

The definition of $\lambda_{eff}$ follows from (11). Since the nuclei, suffering cascade reactions, are left with high excitation energy which is radiated off by evaporation neutrons, we consider $\lambda_{eff}$ to be the parameters describing the longitudinal distribution of the primary neutron source. For lead and uranium we obtain

Pb : $\sigma^{in} \simeq 1.7$ b  $\lambda = 17.8$ cm  $\lambda_{eff} \simeq 28.5$ cm
U : $\sigma^{in} \simeq 1.9$ b  $\lambda = 11.0$ cm  $\lambda_{eff} \simeq 17.6$ cm

b) First Collision Density

We consider as primary neutron source an isotropic line source

$$Q = \frac{Q_o}{2\pi\rho} e^{-z/\lambda_{eff}} \delta(\rho) \tag{12}$$



The first collision density in a cylinder of radius R and length Z is

$$F(r,z) = \frac{1}{Q_o}\int_0^R d\rho\,\delta(\rho)\int_0^Z d\xi\, e^{-\xi/\lambda_{eff}} \frac{\Sigma}{4\pi[(r-\rho)^2+(z-\xi)^2]}$$

$$\exp(-\Sigma\sqrt{[r-\rho]^2+[z-\xi]^2}) = \frac{1}{4\pi Q_o}\int_0^Z d\xi e^{-\xi/\lambda_{eff}}$$

$$\frac{\Sigma}{r^2+(z-\xi)^2} \exp(-\Sigma\sqrt{r^2+[z-\xi]^2}) \tag{13}$$

The collision probability in the cylinder is

$$P = 2\pi\int_0^R rdr \int_0^Z dzF(r,z) \tag{14}$$

These expressions are very sensitive to the cross sections involved. We used spectrum averaged cross sections using the rather hard experimental spallation spectrum ($\bar{E} \simeq 4$ MeV) already quoted[2].

$$\langle\sigma\rangle = \sum_i \left(\frac{dN}{dE}\right)_i \cdot \frac{\sigma(E_i)\Delta E_i}{N} \tag{15}$$

In Fig. 6 we show the spectrum weighted fission and (n,2n) cross section of $^{238}U$. It is readily seen that the high-energy tail of the spectrum contributes strongly to further neutron production by fast fission and (n,2n) reactions. We have now to integrate (13) and (14) using an averaged transport cross section

$\langle\sigma_{th}\rangle = 5.34$ b

leading to an average transport length $\lambda_{th} \simeq 3.9$ cm. The $\xi$-integration in F (r,z) was obtained using an asymptotic expansion of the integrand.A closed approximate expression for F (r,z) followed.

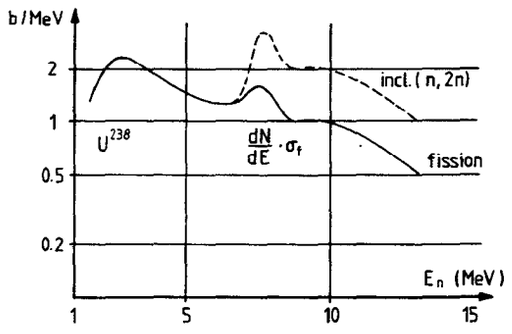


Fig. 6
Spectrum weighted fission and (n,2n) cross section of depleted uranium. The spectrum of Fig. 4 is used.

The collision probability P was obtained by evaluating the further integrals graphically. For an uranium target with a diameter of 15 cm the following first collision probability resulted:

$$P^{238U}_{\bar{E} = 4\ MeV} \quad (R = 7.5\ cm) = 0.8 \tag{16}$$

c) Multiplication Tree

We use the terminology of reactor physics. The number of neutrons from one collision is

$$\eta = \frac{\nu\sigma_f + \sigma_e}{\sigma_{tr}} \tag{17}$$

After n-collisions we have therefore ($P_i$ : collision probability in $i^{th}$ generation),

$$P_1 P_2 \ldots P_n \eta^n \tag{18}$$

fast neutrons. Of these ($\frac{1-P_{n+1}}{\sigma_i/\sigma_{tr}}$ escape go below fission threshold



Hence after the $n^{th}$ generation

$$1 - P_{n+1} + P_{n+1}\,\sigma_i/\sigma_{tr} = 1 - \alpha P_{n+1} \tag{19}$$

neutrons are not useful anymore for fission. Since the spallation neutrons with their hard spectrum are much more efficient for fission reactions than the fission neutrons themselfes, we have to distinguish these two species carefully in the averaging process. The relevant parameters are the following:

| Average over Spallation Spectrum | | Average over Fission Spectrum | |
|---|---|---|---|
| $\alpha_{sp}$ | = 0.59 | $\alpha_f$ | = 0.43 |
| $\eta_{sp}$ | = 0.80 | $\eta_f$ | = 0.52 |
| $P_{2sp}$ | = 0.76 | $P_{2f}$ | = 0.70 |
| $P_1$ | = 0.8 | | |

The first collision probability $P_1$ comes from the previous consideration. $P_2$ is the collision probability for all the further generations assuming, as in the case of the beryllium sleeve, a homogeneous distribution of the neutrons in the cylinder[4]. Following through three generations we obtain a multiplication factor

$$M = 1.45\ \text{Neutrons/Source Neutron} \tag{20}$$

The yield of source neutrons (that is from a thin target) is by a factor of 1.4 higher from uranium than from lead[6]. Hence

$$\text{Yield } (^{238}U) \simeq 2 \times \text{Yield (Pb)} \tag{21}$$

The following critical remark is, however, appropriate. The high-energy tail of the spallation spectrum (E > 15 MeV) has not been considered. In view of the total cross sections at high-energy and the large neutron emission number $\nu$ a higher yield ratio than (21) is expected. Scaling with the total cross section suggests an increase of the yield ratio up to 2.5 to 3.0.

## Conclusions

The task of these investigations is twofold. Firstly, we hope that we figured out a few useful numbers. Secondly, and hopefully more important indeed, it has been shown that these old fashioned methods are still a valuable tool to get some insight into the physics behind the neutronics of the system. This understanding, together with the certainly approximate quantitative results, gives us the confidence to tackle these problems - and more involved ones - with the powerful Monte-Carlo codes most efficiently.



## References

1) С.М. Захарова и др.
Ядерная-физические константы для расчета реакторов
Госатомиздат 1963

2) S. Cierjacks, M. Rainbow, M.T. Swinhoe, L. Buth,
Neutron Yield and Fast Neutron Spectra from Spallation Targets
(presented at this conferency by N. Nücker)

3) R.R. Fullwood, J.D. Cramer, R.A. Haarman, R.P. Forrest,
R.G. Schrandt, LA-4789, Los Alamos 1972

4) Introduction to Neutron Diffusion
K.M. Case, F. de Hoffmann, G. Placzek, Los Alamos 1953

5) M. Barbier, R. Hunter, CERN-71-13, 1971

6) M. Bercovitch et al. Phys.Rev. 119 (1960) 412, and
Р.Г. Василъков и др.
Ядерная физика 7, 88 (1967)